Nano-Diamond compressibility at pressures up to 85 GPa

C. Pantea[*], J. Zhang[*], J. Qian[*], Y. Zhao[*], A. Migliori[*], E. Grzanka[**], B. Palosz[**], Y. Wang[***], T.W. Zerda[***], H. Liu[****], Y. Ding[****], P.W. Stephens[*****] and C.E. Botez [*****]

[*]Los Alamos National Laboratory, Los Alamos, NM, USA
[**]Institute of High Pressure Physics, Polish Academy of Sciences, Warsaw, POLAND
[***]Department of Physics and Astronomy, TCU, Fort Worth, TX, USA
[****]HPCAT-Carnegie Institution of Washington, Advanced Photon Source, Argonne National Laboratory, Argonne, IL, USA
[*****]Department of Physics and Astronomy, SUNY at Stony Brook, Stony Brook, NY, USA

ABSTRACT

The pressure-volume relationship of nano-size diamond was studied at pressures up to 85 GPa. In-situ, monochromatic x-ray experiments, were performed in a diamond-anvil-cell, in a medium that provided pseudo-hydrostatic pressure conditions. Individual peaks were fitted using the Birch-Murnaghan equation-of-state, providing different compressibilities for the surface layer (expanded structure with longer interatomic distances) and the core of the nano-size diamond particles.

Keywords: x-ray, equation-of-state, nano-size, diamond.

1 INTRODUCTION

Materials of micrometer size grains contain on the surface an insignificant fraction of the total number of atoms. Effect of the surface atoms on overall properties of the material can be ignored. However, for nano-size grains the situation is different, due to the fact that the fraction of atoms on the surface is considerable with respect to the total number of atoms. For example, a diamond crystallite with the size of 5 nm has about 50-60% of the total number of atoms on the surface [1].

In nano-size grains, the long-range order is limited by the size of the crystallite, which is smaller than the coherence length of the scattered beam. The values of lattice parameters calculated from individual Bragg reflections are named "apparent lattice parameters", *alp*'s [2]. They are linked to the Q-values of the corresponding reflections ($Q=2\pi/d$). However, there are no existing analytical functions that can simply describe the dependence of alp values on the Q-vector. Therefore, an evaluation of the crystal structure is made based on a comparison of the experimental and theoretical alp-Q relations [1-3].

For a nano-size structure with strained surface shell the alp-Q relation shows a complex dependence with some characteristic minima and maxima. These features can be used for identification and evaluation of the surface structure: (i) the alp values measured at very large Q tend to approach the value of the lattice parameter in the grain core, (ii) "jumps" of alp values calculated for individual reflections are caused by anisotropy of the grain shapes; this effect is strong for very small grains and diminishes with an increase of the grain size [4].

2 METHODS AND MATERIALS

A diamond powder of 0-5 nm in size from Ultradiamond Technologies Inc., *Ultradiamond90*, was used for the present study. The diamond nanoparticles contain 90% diamond. The rest of 10%, consists of graphite and amorphous carbon.

High resolution diffraction experiments, at ambient conditions of pressure and temperature, were performed using (1) neutrons, at the NPDF (Neutron Powder Diffractometer) beamline, Los Alamos Neutron Science Center (LANSCE), Los Alamos National Laboratory, and (2) synchrotron monochromatic x-ray, λ=0.699 Å, at X3B1 beamline, National Synchrotron Light Source (NSLS), Brookhaven National Laboratory (BNL).

I*n situ*, monochromatic x-ray diffraction experiments at high pressures were conducted in a Mao-Bell Diamond Anvil Cell (DAC) at the insertion device beamline 16-ID-B (HPCAT) of the Advanced Photon Source (APS) at Argonne National Laboratory, using a fixed wavelength of 0.422 Å. The x-ray patterns were collected using a charge coupled device (CCD) camera. The maximum pressure achieved was 84.4 GPa. A stainless steel gasket with a sample chamber of 150 μm diameter and 70 μm thickness was used. This gap was filled with powdered nanodiamond and a small quantity of gold, used for pressure calculations, according to the equation of state determined in Ref. 5. Silicone oil was used as a pressure transmitting medium.

In order to differentiate between the pressure effects on the core and the shell of nano-size diamond, the cell volume was calculated as $(alp)^3$ separately for different values of Q. The data were further fitted with the Birch-Murnaghan equation of state

$$p = \frac{3}{2}\cdot K_0 \cdot \left[\left(\frac{V}{V_0}\right)^{-\frac{7}{3}} - \left(\frac{V}{V_0}\right)^{-\frac{5}{3}}\right]\cdot\left[1-\frac{3}{4}\cdot\left(4-K_0^{'}\right)\cdot\left(\frac{V}{V_0}\right)^{-\frac{2}{3}}-1\right] \quad (1)$$

where p is the pressure, V_0 is the molar volume at ambient conditions, V is the volume at a certain pressure p, and K_0 and K'_0 the isothermal bulk modulus and its pressure derivative at 300 K, respectively. The bulk modulus for different reflections was determined separately for the up-stroke and down-stroke cycles, and for the both cycles together.

3 RESULTS

A typical x-ray diffraction pattern is shown in Figure 1a. The integrated x-ray diffraction patterns were fitted by the Grams package, together with the background subtraction, for further refinement of the cell parameters. A typical refined pattern is shown in Figure 1b.

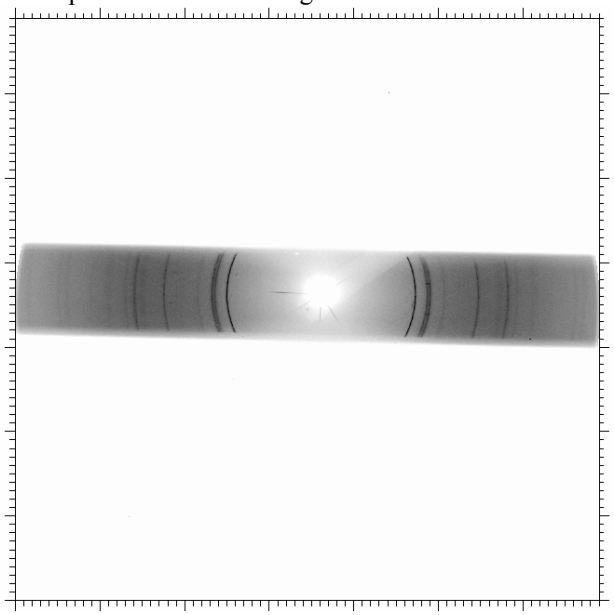

a.

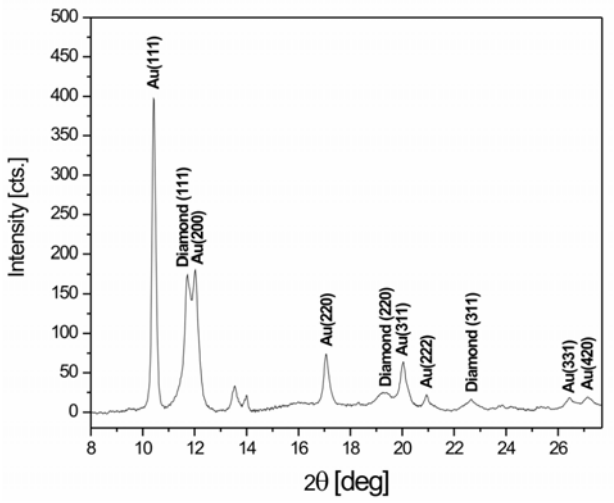

b.

Figure 1: a. Typical diffraction pattern at high pressure. b. Plot of the reduced x-ray diffraction pattern at a pressure of 8 GPa.

In Fig. 2 the *alp* vs. *Q* graph is shown for diamond of different crystallite sizes. It can be observed that the deviation of alp values from those of bulk diamond (illustrated by a straight line) becomes more significant as grain size decreases. The experimental errors are small and the fluctuations in the *alp* values reflect real effects. The *alp* values critically depend on how the crystal was cleaved and on Miller indices of the diffracting planes. Small Q-values are characteristic to the surface shell, while high Q-values correspond to the inner core of the nanosize crystals. It is seen that the structure of outer layers of nano-size diamonds is not as dense as that of the core, which is in very good agreement with TEM results. As expected, for large crystals this effect is negligible.

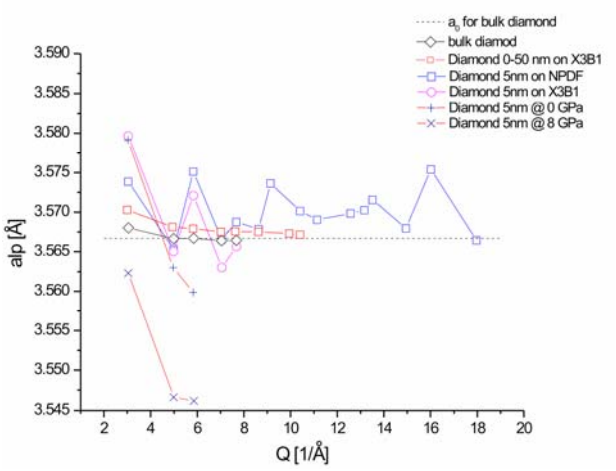

Figure 2: alp vs. Q plot for diamond powders of different sizes, and for the 5 nm diamond at high pressure.

In order to understand the changes induced by pressure in nano-size diamonds, TEM images (Figure 3) were obtained for a nano-size diamond powder of 0-50 nm, which was sintered at p = 8.0 GPa, T = 1470 K, for 60 s, without using a pressure transmitting medium (Figure 3). After treatment the diamond crystals were smaller than the initial powder. High pressure used during sintering caused numerous fractures, and therefore reduced the average crystal size (see for example the image segment marked with (2) in Figure 3b). It can also be seen that the bonds between Carbon atoms situated close to the grain surface are highly distorted. At grain contacts, diamond particles are pressed one into another, indicating the presence of significant amount of stresses. Atoms close to the surfaces would rearrange to accommodate the stresses from the surface, forming highly distorted bonds, see Figure 3b, image segment marked with (1). The strains present in the distorted C-C bonds are pressure and temperature dependent [6,7] with strains increasing with applied pressure. It should be mentioned that these results are obtained from samples recuperated from the high pressure – high temperature (HPHT) cell, i.e., after the pressure and temperature were released. It is safe to assume that under high pressure the strains are higher.

Another important conclusion of the TEM analysis is that nanocrystals are clearly composed of two distinctly different regions. Interior of the crystals shows ordered crystallographic structure composed of flat surfaces, while the outer layers include curved surfaces and high concentration of amorphous structures. After HPHT treatment concentration of amorphous structures appears to be reduced. Such interpretation is not objective or quantitative. More reliable data on changes induced by pressure on the structure of nanosize diamond can be obtained using x-ray scattering in a diamond anvil cell.

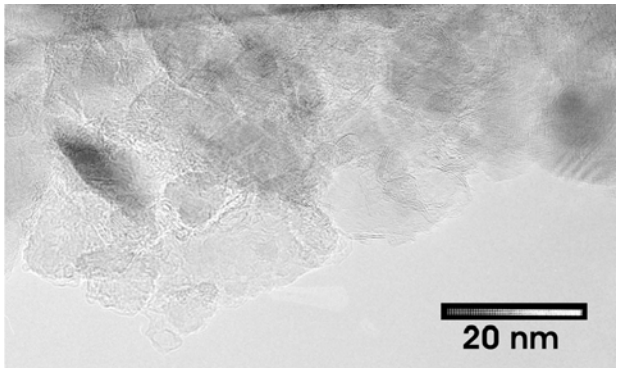

a.

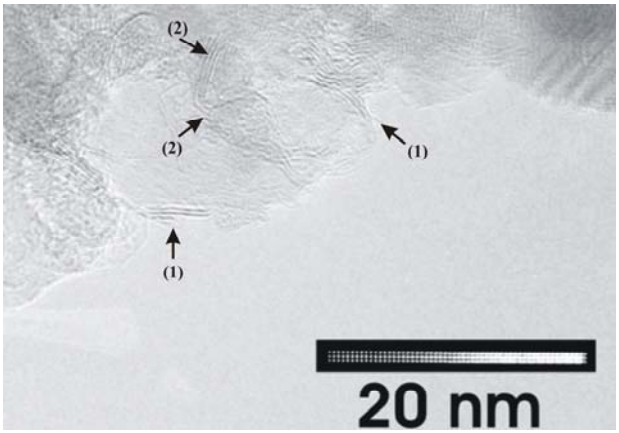

b.

Figure 3: a. TEM of diamond powder with size of 0-50 nm after sintering at 8.0 GPa and 1470 K for 60 seconds; b. magnification of a region of interest in Figure 4a.

The *alp*'s obtained for different nano-diamond reflections were used to calculate the so-called *apparent* V/V_0, which was further fitted using the second-order Birch-Murnaghan equation of state. An example for the (111) reflection of nano-diamond is shown in Figure 4. The estimated bulk moduli for different reflections are summarized in Figure 5. Because of the limitations imposed by the experimental setup, we were able to investigate only the first three peaks of nano-size diamond, i.e (111), (200), and (220).

The bulk modulus was calculated using a K_0'=4.0, mainly due to the scatter in data for the peaks corresponding to nano-size diamond at high pressures, and overlap with the peaks of the pressure calibrant (gold), see Figure 1. In Figure 5 the data are presented for the increasing pressure cycle (grey Δ), for the decreasing pressure cycle (black ∇), and for the average of the up and down cycle (red o). We were unable to distinguish the (220) peak corresponding to nano-size diamond from the background for the decreasing pressure cycle.

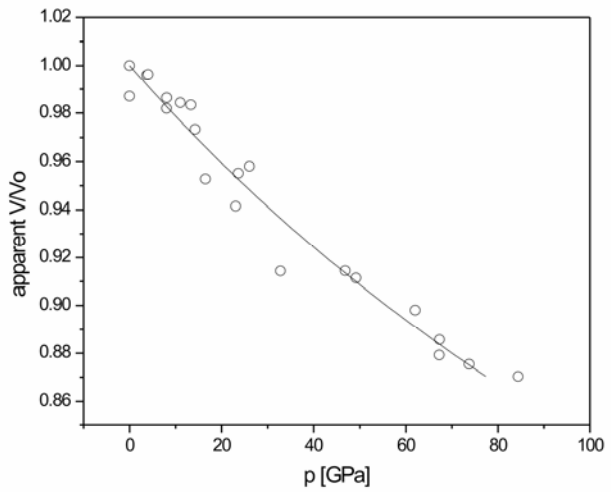

Figure 4: Variation of apparent V/V_0 for the (111) peak of nano-diamond as a function of pressure.

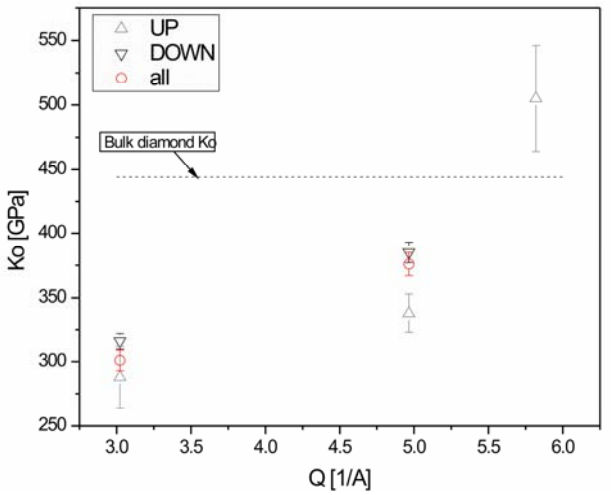

Figure 5: Bulk modulus vs. scattering vector Q, obtained for individual reflections of diamond 5 nm.

The present experimental results (Figure 5) demonstrate that the outer shell of the nano-size diamond has a much lower bulk modulus than bulk diamond, i.e. 300 GPa vs. 442 GPa. As the inner core inner core is probed by the incident x-ray beam, the bulk modulus derived from the diffraction increases noticeably, up to about 500 GPa. Figure 5 also reveals that the compressibility (the reciprocal of bulk modulus) corresponding to large Q reflections is smaller than that obtained for small scattering vector *Q*. In other words, the shell can be compressed more readily than

the interior of the grain. Such a difference in compressibility of the shell and the core suggests that more strains develop in the shell.

4 CONCLUSION

According to the core-shell model [1,2,8] nanocrystals consist of a uniform core surrounded by a surface shell. Crystallographic structure of the surface shell is the same as that of the core but interatomic distances in the surface layer are different than those in the center of the crystal. For diamond the surface layer has a slightly expanded structure with longer interatomic distances [1,2], and the interior and exterior regions of nanocrystals have noticeable different compressibilities.

The outer shell of the nano-size diamond has a much higher compressibility in comparison with bulk diamond, reflected in smaller value for the bulk modulus. The compressibility is decreasing rapidly with the scattering vector Q, resulting in a smaller compressibility for the inner core in comparison with the surface layers of the nano-size diamond particles.

ACKNOWLEDGMENTS

This research was partly supported by the Polish Ministry of Education and Science, grant 3 T08A 020 29 (EG & BP), and under the auspices of the U.S. Department of Energy (DOE) under contract W-7405-ENG-36 with the University of California. The experimental work was performed at HPCAT (Sector 16), Advanced Photon Source (APS), Argonne National Laboratory. Use of the HPCAT facility was supported by DOE-BES, DOE-NNSA (CDAC), NSF, DOD–TACOM, and the W.M. Keck Foundation. Use of the APS was supported by DOE-BES, under Contract No. W-31-109-ENG-38. This work has benefited from the use of NPDF at the Lujan Center at Los Alamos Neutron Science Center, funded by DOE Office of Basic Energy Sciences and Los Alamos National Laboratory funded by Department of Energy under contract W-7405-ENG-36. The upgrade of NPDF has been funded by NSF through grant DMR 00-76488. Research also carried out in part at the National Synchrotron Light Source at Brookhaven National Laboratory, which is supported by the US Department of Energy, Division of Materials Sciences and Division of Chemical Sciences. The SUNY X3 beamline at NSLS is supported by the Division of Basic Energy Sciences of the US Department of Energy under Grant No. DE-FG02-86ER45231.

REFERENCES

[1] B. Palosz, E. Grzanka, S. Gierlotka, S. Stel'makh, R. Pielaszek, U. Bismayer, J. Neuefeind, H. P. Weber, T. Proffen, R. Von Dreele and W. Palosz, Z. Kristallogr. 217, 497, 2002.

[2] B. Palosz, S. Stel'makh, E. Grzanka, S. Gierlotka, R. Pielaszek, U. Bismayer, S. Werner, and W. Palosz, J. Phys.: Condens. Matter 16, S35, 2004.

E. Grzanka, S. Gierlotka, S. Stelmakh, R. Pielaszek, W. Lojnowski, U. Bismayer, J. Neuefeind, H.P. Weber and W. Palosz, Phase Transitions 76, 171, 2003.

[3] B. Palosz , E. Grzanka, S. Gierlotka , S.Stel'Makh , R. Pielaszek , U. Bismayer, J. Neuefeind , H.P. Weber and W. Palosz, Phys. Pol. A 102, 57, 2002.

[4] B. Palosz, E. Grzanka, C. Pantea, T.W. Zerda, Y. Wang, J. Gubicza and T. Ungar, J. Appl. Phys. 97, 064316, 2005.

[5] D.L. Heinz and R. Jeanloz, J. Appl. Phys. 55, 885, 1984.

[6] C. Pantea, J. Gubicza, T. Ungar, G.A. Voronin, T.W. Zerda, Phys. Rev. B 66, 094106, 2002.

[7] C. Pantea, J. Gubicza, T. Ungar, G.A. Voronin, N.H. Nam, T.W. Zerda, Diam. Relat. Mater. 13, 1753, 2004.

[8] H. Gleiter, Acta Mater. 48, 1, 2000.